Journal of Applied Mechanics and Technical Physics, Vol. 35, No. 5, 1994

STRUCTURE OF THE PLASMA JET OF A PULSED EROSIONAL ELECTRIC-DISCHARGE SOURCE

S. B. Leonov and G. A. Luk'yanov

UDC 533.9.082.5

The gas-dynamic structure of the plasma jet of a pulsed electric-discharge source depends essentially on the geometrical and electrical parameters of the source, the conditions of plasma outflow from the nozzle, and the parameters of the ambient medium. The varied combinations of these parameters and conditions determine the rather large variety of flow structures of such jets. In the initial section of the jet, the character of the flow is strongly affected by such specific features of the electric-discharge source as the bulging of electric current beyond the nozzle cut and the great nonuniformity of the parameters at the nozzle cut of the source, associated with plasma-generating matter coming from the nozzle walls and other circumstances. The complexity of the outflow pattern demands great caution in applying to such jets the conclusions obtained for other types of jets (such as pulsed gas jets or steady jets of electric-discharge sources with gaseous working substances) [1]. The experimental study of pulsed plasma jets, on the whole, has not yet reached the level at which fairly broad generalizations are possible. Most research has been of a particular nature. Of the most significant experimental papers on the study of plasma jets of this type, we can note [2, 3].

In the present paper we investigate the structure and parameters of an erosional plasma jet generated by a pulsed electric-discharge source with a cylindrical discharge channel and escaping into a filled space (still air under standard conditions) at an expansion ratio $n = p_a/p_\infty$ close to unity (p_a is the pressure at the nozzle cut and p_∞ is the ambient pressure).

The construction of the plasma source is given in Fig. 1. The source consists of a graphite cathode 1, a dielectric insert 2 of polymethyl methacrylate (PMMA), which is simultaneously the source of the working substance owing to vaporization of the walls of the discharge channel, and a multisectioned copper anode 3 (to eliminate an anode flame, the discharge current is distributed over the 10-20 anode sections by ballast circuits). The plasma source was supplied from a capacitive storage with pulling inductances. The typical forms of the discharge current and the voltage U on the electrodes are given in Fig. 2.

The following parameters of the plasma source are typical for these experiments: diameter of discharge channel $d = 0.5$-4 mm, length of discharge channel $l = 3$-15 mm, discharge current at the maximum $I = 280$-1500 A, duration of a discharge pulse $\tau = 1$-8 msec, average flow rate of the plasma-producing substance, determined by weighing, $G = 0.1$-4 g/sec, mass-averaged stagnation enthalpy (determined from the average applied power P) $h = (5\text{-}10)\cdot 10^7$ J/kg. The outflow conditions corresponded to Reynolds numbers $Re = 4G/\pi d\mu = 10^3\text{-}10^4$ and a degree of ionization $\alpha = 0.1$-0.9. The viscosity μ and the degree of ionization were found at standard pressure and the mass-averaged stagnation temperature. The typical regimes of the plasma source and conditions of jet outflow are characterized in Table 1.

Measurement Method. To obtain information about the flow pattern and parameters in these experiments, we used the following methods: photography integrated over time, high-speed photograph scanning (including a time-loop regime with a 10-50 μsec exposure per frame), the direct-shadow method, the Töpler method, and the method of defocussed diaphragms [4] with a 20 nsec exposure time. A Zenit mirror camera was used in the first case, an SFR-1M streak camera in the second, and a laser instrument with an active element based on aluminum–yttrium garnet with neodymium and with radiation frequency doubling, with modulation of the resonator quality, similar to the instruments described in [5], was used in the shadow methods. The gas flow velocity was calculated from the slope of the lines of propagation of plasma inhomogeneities on the streak camera recordings by the standard method.

St. Petersburg. Translated from Prikladnaya Mekhanika i Tekhnicheskaya Fizika, No. 5, pp. 13-18, September-October, 1994. Original article submitted July 28, 1993.

0021-8944/94/3505-0653$12.50

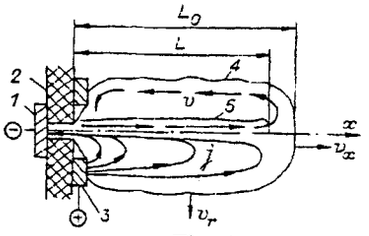

Fig. 1

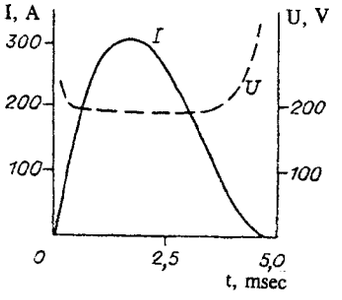

Fig. 2

The plasma temperature at the jet axis was determined using a single electrostatic probe, and the radial temperature distribution of neutral particles in the axial region was determined from the relative intensities of vibrational–rotational bands of the violet system of cyanogen bands [6], with conversion from integrated to local characteristics using regularizing algorithms [7]. The electron density near the jet axis was measured from the Stark broadening of the Hβ hydrogen line [8]. The measurements showed that the temperatures of electrons and heavy particles beyond the nozzle cut of the source for different regimes are in the range $(10\text{-}20)\cdot 10^3$ K.

Flow Pattern. The process of generation and outflow of the plasma jet can be divided arbitrarily into four stages: breakdown, initial stage, quasisteady stage, and decay.

The electric discharge begins with a high-voltage breakdown in the gap bounded by the dielectric. Heating of the wall of the discharge channel causes vaporization of the material of the dielectric insert. The gas in the channel is heated by the electric current flowing through it. The pressure increase resulting from the heating leads to the establishment of a gas stream from the nozzle of the source.

Diagrams of the flow in the initial and quasisteady stages are given in Figs. 1 and 3. The direct-shadow and Töpler photographs enable one to observe distinctly the contact boundary 4 (Fig. 1) separating the escaping gas from the ambient medium. At the flow axis there is a brightly luminous region 5 of almost cylindrical geometry. The plasma in this region moves at a high velocity and has a high specific enthalpy. In Fig. 1 we also give a qualitative picture of the spread of electric current density j in the jet (lower part) and of the plasma motion with velocity v (upper part). In the course of the experiments, the boundary, clearly observed in photographs, which are not given here, of the high-enthalpy axial region corresponds to the zone of large plasma temperature and density gradients, with a radial thickness of about 2-3 mm. Over this distance the temperature decreases at least twofold with distance from the axis, while the degree of ionization decreases by about an order of magnitude.

In the initial stage of outflow, the high-enthalpy axial stream reaches the contact boundary and flows out radially, and then turns around and moves back toward the nozzle of the source. The region between the high-enthalpy core and the contact boundary forms a kind of envelope around the axial flow, filled with the outflowing plasma. The density in this envelope is considerably lower than the ambient gas density. In the initial stage, the length L of the high-enthalpy stream and the length L_0 of the plasma envelope increase at the same, almost constant velocity. In Fig. 4 we give experimental data on the axial and radial velocities of the contact boundary for regime 2.

After a certain time (1-1.5 msec after breakdown), the length L of the high-enthalpy core ceases to increase, while the size of the plasma envelope continues to grow. It is natural to take the time at which the high-enthalpy axial stream reaches its greatest length as the end of the initial outflow stage. A diagram of the flow in the quasisteady stage of outflow is given in Fig. 3. In the quasisteady stage, the plasma envelope expands uniformly in all directions. This is indicated by the equalization of the velocities of the contact boundary in the axial and radial directions at $t > 1.5$ msec (Fig. 3). A spherical region develops in the head part of the plasma envelope. Large-scale gas motion (like a Wood's ring) is formed inside this region, which remains stable after the discharge ends and is detected from its self-emission for several or even tens of milliseconds.

Analysis of Results. The plasma velocity at the jet axis as a function of the relative distance $x^0 = x/d$ to the nozzle of the source for regimes 2-4 is given in Fig. 5. The measurements showed that the plasma velocity is virtually constant within the high-enthalpy, brightly luminous core of the jet, and then it falls off rapidly. In accordance with the schematization adopted in the gas dynamics of jet flows, the constant-velocity section of the jet beyond the nozzle of the source is called the initial section of the jet [1]. The high-enthalpy core of the jet is thus its initial section. The relative length L/d of the initial section for different regimes is given in Table 1. The experiments showed that L/d has a considerable statistical scatter in repeated

TABLE 1

Regime	l, mm	d, mm	I, A	G, g/sec	P, kW	τ, msec	h, 10^7 J/kg	L/d	M
1	15	3÷4	300	1,0	57	4.2	5.7	10÷30	≤1
2	10	2÷2,5	305	0.5	34	4.5	6.8	30÷80	≤1
3	15	3÷4	850	2.2	135	2.6	6.0	10÷30	>1
4	15	3÷4	1500	4	250	1.2	6.2	10÷20	>1
5	3	0,5÷1	280	0,15	15	6	10	200÷600	~1
6	4	1÷1,5	1500	1,0	87	1.5	8.7	50÷100	~1

firings of the source for one regime and may vary considerably even during one discharge. In our opinion, this instability is due to fluctuations of the bulging currents.

Both supersonic (a Mach number $M \simeq 1$ at the channel exit of the source) and subsonic ($M < 1$) regimes of outflow were observed in the experiments. In the supersonic regimes, a typical shock-wave structure occurs in the initial section of the jet, including one or several "barrels" [1]. Regimes 1 and 2 in Table 1 correspond to $M < 1$ and to subsonic flow beyond the nozzle of the source in the initial and quasisteady stages of outflow. Regimes 3 and 4 correspond to supersonic flow in the initial section of the jet in the part of the initial and quasisteady stages of outflow when the discharge current is sufficient to create a supercritical pressure drop between the source chamber and the ambient space. During the growth and decay of the discharge current in these regimes, the jet successively passes through the stages of subsonic, supersonic, and again subsonic outflow.

As the current grows, the subsonic initial section is replaced by a supersonic one with a periodic "multibarrel" shock-wave structure, which corresponds to the range of expansion ratios $1 < n < 2$ [1]. A further increase in the discharge current leads to an increase in n and a gradual decrease in the number of "barrels" to one. In the photographs and streak camera recordings for regimes 5 and 6 with the highest specific enthalpy, no shock-wave structure is observed. The visible flow pattern and estimates of the Mach number in the initial section for these regimes indicate the closeness of the flow in the initial section to sonic flow.

Let us consider the experimental data on the length of the initial section of the jet in the quasisteady expansion stage. The end of the subsonic section and the supersonic initial section correspond to closure at the jet axis of the layer in which the gas flowing out of the source mixes with the ambient gas. In the pulsed jets under consideration, the role of the ambient medium is played by the gas filling the plasma envelope. In supersonic outflow from the source, in contrast to subsonic jets, the velocity in the initial section does not remain constant, in general, but varies in accordance with the geometry of the shock-wave structure [1]. Only in the special case in which $n = 1$ is the velocity at the axis constant within the initial section. The supersonic outflow regimes 3 and 4 in Fig. 5 correspond to values of n close to unity, when the intensity of the shocks in the initial section is relatively low. The latter explains the absence of noticeable (exceeding the measurement error) velocity changes within the initial section in these regimes.

For supersonic, steady, submerged gas jets with a small expansion ratio ($n \lesssim 2$) in a turbulent flow regime, the length of the initial section is determined from the empirical equation [9]

$$L/d = 9.5[M\sqrt{n\gamma} - 1.05/(M\sqrt{n\gamma})^{2.7}].$$

For $M = 1$, $n = 1$-2, and $\gamma = 1.1$-1.5, we have L/d = 10-15. Similar results have been obtained in experiments with plasma jets from steady electric-arc plasmatrons in outflow from sonic nozzles with $n < 2$ in a laminar flow regime [1].

The results of these experiments on the determination of L/d are given in Table 1 and in Fig. 6. The experimentally observed values of the relative length of the initial section in the quasisteady stage of outflow for regimes 1, 3, and 4 are in satisfactory agreement with our present understanding. For the higher-enthalpy regimes, the results proved to be rather unexpected. Flow in the narrow axial region of the jet in regime 5 is maintained with an almost constant velocity over a distance of several hundred diameters of the nozzle of the source.

Let us discuss qualitatively the physical nature of the formation of an anomalously long initial section or an anomalously "long range" of a high-enthalpy pulsed jet. In our opinion, the reason for the anomalously "long range" of jets in high-enthalpy regimes is the sharp decrease in plasma viscosity at $T > 10^4$ K, resulting in a corresponding decrease in

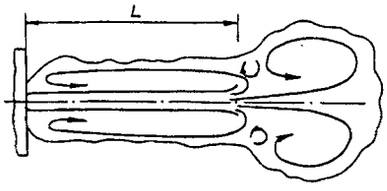

Fig. 3

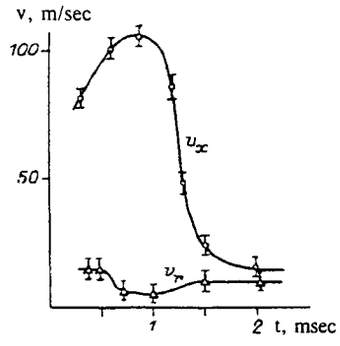

Fig. 4

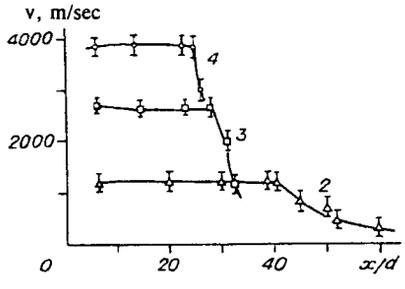

Fig. 5

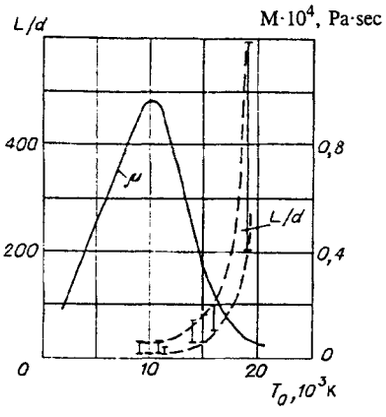

Fig. 6

viscous dissipation in the jet's axial region and elongation of the initial section. In Fig. 6 we have plotted L/d as a function of stagnation temperature T_0, determined under the assumption of thermodynamic equilibrium from the experimental value of h using the data of [10]. In Fig. 6 we also give the temperature dependence of the viscosity μ of PMMA (plastic) at standard pressure. In the temperature range corresponding to a low degree of ionization ($\alpha < 3\cdot10^{-2}$), we have $\mu \sim T$. At $\alpha > 3\cdot10^{-2}$, collisions between atoms and ions, accompanied by charge exchange and having larger effective collision cross sections, begin to play the main role in momentum transfer. A sharp decrease in viscosity (approximately 40-fold) is observed in the range $T = 10^4$-$2\cdot10^4$ K. With a further increase in T and α, the viscosity is determined by ion−ion collisions and increases monotonically with increasing T ($\mu \sim T^{5/2}$). The data given in Fig. 6 indicate a clear-cut correlation in the temperature dependences of L/d and μ.

Obtaining a temperature $T \simeq 2\cdot10^4$ K at the output from the source, corresponding to the high-temperature minimum of viscosity in the function $\mu = \mu(T)$, is a necessary condition for achieving the effect of anomalously "long range" of the jet. Another determining condition is the presence of a sufficiently dense bulging current, providing for Joule heating of the plasma in the axial region of the jet. In the investigated range of parameters of the source and of outflow regimes, the effect of anomalously "long range" occurs at current densities $j > 10^8$ A/m^2 in the discharge channel. In this range of j, the approximating empirical function

$$L/d \simeq 0.5\cdot10^{-6}I/d^2$$

is valid, where I is the current in amperes and d is the diameter in meters. A third essential condition for obtaining a "long range" is a transonic flow regime in the initial section. In this case, sufficiently high axial impulses are achieved, which determine the velocity of the head part of the plasma envelope in the initial stage of outflow. In jets of the type under consideration these factors interact in such a way that when the temperature corresponding to the high-temperature minimum of viscosity is reached at the exit from the source, a stable gas-dynamic structure with an anomalously long initial section is

formed beyond the nozzle. Such a structure obviously can exist only during a time limited by the period of existence of the plasma envelope.

The authors thank I. A. Sokolova for the data she provided on the viscosity of a PMMA plasma.

REFERENCES

1. G. A. Luk'yanov, Supersonic Plasma Jets [in Russian], Mashinostroenie, Leningrad (1985).
2. L. Ya. Min'ko, Obtaining and Investigating Pulsed Plasma Streams [in Russian], Nauka Tekhnika, Minsk (1970).
3. L. I. Kisilevskii, V. A. Morozov, and V. N. Snopko, "Properties and application of pulsed, high-enthalpy, supersonic plasma jets," in: Physics and Application of Plasma Accelerators [in Russian], Nauka Tekhnika, Minsk (1974).
4. L. A. Vasil'ev, Schlieren Methods [in Russian], Nauka, Moscow (1968) [translated by A. Baruch, Keter Inc., New York (1971)].
5. A. N. Zaidel' and G. V. Ostrovskaya, Laser Methods in Plasma Research [in Russian], Nauka, Leningrad (1977).
6. Optical Pyrometry of a Plasma [Russian translation], N. N. Sobolev (ed.), Gos. Izd. Inostr. Lit., Moscow (1963).
7. Yu. E. Voskoboinikov, N. G. Preobrazhenskii, and A. N. Sedel'nikov, Mathematical Experiment Analysis in Molecular Gas Dynamics [in Russian], Nauka, Novosibirsk (1984).
8. Plasma Diagnostic Techniques, R. H. Huddlestone and S. L. Leonard (eds.), Academic Press, New York (1965).
9. P. A. Neshcheret, E. A. Kapustin, and O. É Shlik, "Calculation of flow in the main section of a supersonic jet with allowance for the influence of the end of the nozzle," Prikl. Mekh. Tekh. Fiz., No. 5 (1984).
10. Yu. V. Boiko, Yu. M. Grishin, A. S. Kamrukov, et al., Thermodynamic and Optical Properties of Metals and Dielectrics [in Russian], Metallurgiya, Moscow (1988).